J Appl Electrochem
DOI 10.1007/s10800-015-0854-8

RESEARCH ARTICLE

Enhanced performance of direct ethanol fuel cell using Pt/MWCNTs as anodic electrocatalyst

L. C. Ordóñez[1] · B. Escobar[1] · R. Barbosa[2] · Y. Verde-Gómez[3]

Received: 6 February 2015 / Accepted: 18 May 2015

Abstract Platinum nanoparticles with a size distribution ranging from 3 to 6 nm were synthesized at room temperature by chemical reduction of platinum chloride, using $NaBH_4$ as the reduction reagent and poly(*N*-vinylpyrrolidone) as the stabilizer. The Pt colloidal nanoparticles obtained were deposited onto multi-walled carbon nanotubes (MWCNTs) synthesized by the chemical vapor deposition method. Pt/MWCNTs prepared with a metal content of 20 wt% was evaluated as the anode electrocatalyst in a 9 cm^2 direct ethanol fuel cell using PtRu/C as the cathode material. Both electrodes had a metal loading of 1 mgPt cm^{-2}. Polarization curves showed higher electroactivity for Pt/MWCNTs than commercial material (Pt/C).

Graphical Abstract

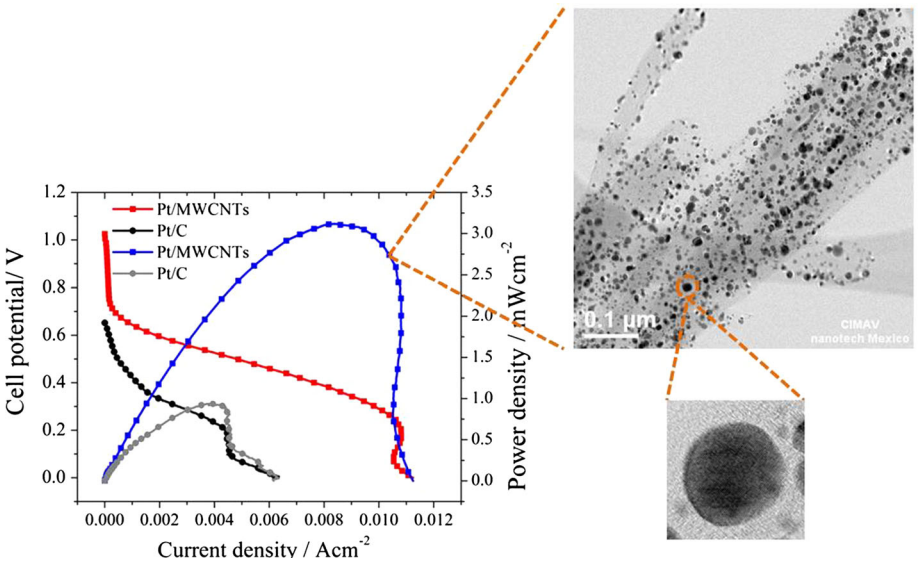

Keywords MWCNTs · Pt/MWCNTs · Ethanol electrooxidation · Direct ethanol fuel cell

✉ Y. Verde-Gómez
ysmaelverde@yahoo.com

[1] Unidad de Energía Renovable, Centro de Investigación Científica de Yucatán, C 43 No 130, Chuburná de Hidalgo, 97200 Mérida, Yucatán, Mexico

[2] Universidad de Quintana Roo, Boulevard Bahía s/n, 77019 Chetumal, Quintana Roo, Mexico

[3] Instituto Tecnológico de Cancún, Av. Kábah Km. 3, 77500 Cancún, Quintana Roo, Mexico

1 Introduction

Direct ethanol fuel cells (DEFC) based on a polymer electrolyte membrane (PEM) are attractive alternative devices for transport and portable applications because of their high thermodynamic efficiency and the ease of

Published online: 04 June 2015

production, distribution, and handling of this low-molecular-weight alcohol [1]. Additionally, ethanol has proven to have a lower crossover rate and reduced cathode performance effects compared with methanol [2]. Under acidic conditions, platinum presents the highest activity for the ethanol oxidation reaction, and it has therefore been used extensively as an anodic catalyst during the past decade [3–6]. However, DEFC commercial applications still have some challenges to overcome, such as intermediate species tolerance and long-term performance. Improved electrocatalytic behavior for the ethanol electro-oxidation reaction essentially depends on three factors: (1) the preparation procedure plays a crucial role in electrocatalyst composition and structure, especially in the interaction between their different components, hence its interaction with the produced species during reaction; (2) a homogeneous dispersion of the active phase is essential in order to ensure high catalytic activity; and (3) smaller particle size is expected to reduce the amount of Pt usage in the catalyst layer without decreasing DEFC efficiency. Several carbon materials with high surface area such as Vulcan XC-72R, single-walled carbon nanotubes (SWCNTs), multi-walled carbon nanotubes, carbon fibers, and aerogels have been investigated as support materials [7, 8]. In proton exchange membrane fuel cell (PEMFC) applications, the deposition of Pt metal nanoparticles onto carbon nanotubes has resulted in higher catalytic activity compared with carbon black-supported materials [9, 10]. However, high dispersion of Pt nanoparticles with controlled loading remains a challenge due to the inert surfaces of MWCNTs [7]. Yang et al. [11] synthesized Pt nanoparticles with a size of between 2 and 4 nm and achieved high dispersion on MWCNTs using the thiolation method via π–π interaction and subsequent thermal treatment. Their results indicated that the synthesized Pt/MWCNTs composite has excellent electrocatalytic activity for methanol oxidation and good CO tolerance. Liu et al. [12] synthesized Pt nanoparticles with an average size of 4 nm, supported on MWCNTs via potentiostatic deposition in a solution bath without adding supporting electrolyte. This material exhibited higher electrocatalytic activity for the ethanol oxidation reaction and better anti-poisoning behavior compared with a commercial Pt/C electrocatalyst. Using the EG reduction method, Jiang et al. [13] obtained Pt nanoparticles with a very narrow size distribution supported on MWCNTs functionalized by plasma treatment. This material presented good performance for ethanol electro-oxidation in a basic solution in comparison with Pt/C. They explained their results on the basis of good metal utilization caused by a strong interaction between the metal and MWCNTs, and good conservation of the tube structure by the plasma treatment. Cai et al. [14] prepared a Pt catalyst supported on MnOx-CNT by the microwave-assisted polyol method. The particles obtained had an average diameter of 2.2 nm and showed good dispersion on the support material. The presence of MnOx in the electrocatalyst promotes the dehydrogenation steps in the ethanol oxidation mechanism, removes the adsorbed intermediates to release the Pt active sites, and then increases Pt utilization via the synergistic effect between Pt and MnOx. Rodríguez et al. [15] synthesized Pt–Fe nanoparticles supported on MWCNTs with an average particle size of between 1.5 and 2.1 nm. The Pt–Fe/MWCNTs electrocatalyst showed high electrocatalytic activity for the methanol oxidation reaction due to the addition of iron. The promoting effect of Fe was related to the adsorption of OH^- species on the electrocatalyst surface at lower potentials than Pt/C.

In this study, we compare the activity for the ethanol electro-oxidation reaction of a commercial Pt/C catalyst and a Pt catalyst supported on MWCNTs synthesized in-house by a modified chemical vapor deposition method (MCVD). The catalyst characterizations were performed by cyclic voltammetry (CV), scanning electron microscopy (SEM), transmission electron microscopy (TEM), and X-ray diffraction (XRD). Finally, the anode catalyst was tested in a direct ethanol fuel cell with an active electrode area of 9 cm^2. The results indicate that Pt/MWCNTs show good behavior under DEFC conditions.

2 Experimental

2.1 Synthesis of carbon nanotubes and Pt/MWCNTs electrocatalyst

The carbon nanotubes were synthesized by the MCVD method at 900 °C using toluene as the carbon source and ferrocene ($Fe(C_5H_5)_2$) as the catalytic agent, as reported elsewhere [16]. The processes for cleaning and functionalization of MWCNTs were performed by refluxing them in a 30 % H_2O_2 solution (2 h) and then in HNO_3 (24 h) at 100 °C. Finally, they were washed thoroughly with triple distilled water. Colloidal dispersions of Pt nanoparticles were prepared by mixing platinum tetrachloride in methanol using poly(*N*-vinyl-2-pyrrolidone) and $NaBH_4$ solution as capping and reducing agents, respectively. A dark brown stable colloid was formed [17].

Pt/MWCNTs was prepared according to the methodology presented previously [18]. Briefly, 100 mg of MWCNTs were dispersed in methanol with strong ultrasonication for 1 h. Pt colloidal dispersion was then added and vigorously stirred for 30 min. Subsequently, the dispersion was dried until complete evaporation. Pt/MWCNTs with a metal loading of 20 wt% was obtained. The catalytic response for ethanol oxidation was compared with commercial 20 wt% Pt/C (AlfaAesar).

2.2 Physical characterization

X-ray diffractograms (XRD) were recorded with a Bruker AXS D8 Advance and a Panalytical Xpert diffractometer using Cu Kα radiation (1.5406 Å) at 40 kV and 40 and 30 mA, respectively. The scanning angle 2θ was varied from 20° to 80° at 0.1°min^{-1}. High-resolution scanning electron microscopy (HRSEM) analyses were performed with a JEOL JSM-7401F field emission SEM operated at low voltage. In order to obtain information on the distribution of Pt nanoparticles supported on MWCNTs, high-resolution transmission electron micrographs were obtained with a JEOL JEM-2200FS transmission electron microscope at 200 kV.

2.3 Electrochemical measurements

Cyclic voltammetry (CV) experiments were carried out at 25 °C in a typical electrochemical three-electrode cell using an Autolab PGSTAT302 potentiostat/galvanostat. Mercury/mercurous sulfate electrode ($Hg/Hg_2SO_4/K_2SO_4$ (sat)) and graphite bar were used as reference and auxiliary electrodes, respectively. The working electrode was prepared by mixing the appropriate amounts of catalyst powder with isopropanol and 5 wt% Nafion® solution. This suspension was ultrasonicated for 15 min. 5 μL of this dispersion was deposited onto a graphite carbon disk electrode (5 mm diameter) using a micropipette. Electrode catalyst loading was 2.54 mg cm^{-2}, expressed in terms of the geometric surface area of the disk.

All electrode potentials are presented with respect to the normal hydrogen electrode (NHE) scale. Prior to electrochemical tests, the catalytic materials were activated in a nitrogen-outgassed 0.5 M H_2SO_4 electrolyte by potential cycling from 0.1 to 1.0 V versus NHE at a scan rate of 100 mV s^{-1} until no changes in electrical current were registered. To observe the complete processes of ethanol oxidation, CV tests were carried out in a potential window from 0.0 to 1.5 V versus NHE at a scan rate of 50 mV s^{-1} [19]. The system was maintained without stirring and all potential sweeps were first carried out towards positive potentials, and then reversed towards negative potentials. The catalytic active area was calculated from the electrical charge of the proton adsorption–desorption CV region, which corresponds to 0.210 mC cm^{-2} [18, 20], and normalized to the catalyst content. Finally, the working solution consisted of 1.0 M ethanol +0.5 M H_2SO_4.

2.4 MEA preparation and performance evaluation in a DEFC

Electrodes were prepared by brushing the catalyst suspension onto commercial diffusers of 9 cm^2 (3 × 3 cm) based on carbon papers. DGS1120 and P75T carbon paper were used for anode and cathode, respectively, both from Ballard®. A catalyst loading of 1 mgPtcm^{-2} of PtRu/C electrocatalyst (Alfa Aesar) was deposited on the cathode, while a catalyst loading of 1 mgPt cm^{-2} of Pt/MWCNTs or commercial Pt/C electrocatalyst was deposited on the anode. Nafion ® 117 membrane was used as electrolyte. The assembly was fabricated by the hot pressing method at 4000 lbin and 120 °C. The single cell was fed with a 1.0 M aqueous ethanol solution at 1.5 mL min^{-1}. On the cathode side, air was supplied at 140 mL min^{-1}.

3 Results and discussion

3.1 Materials characterization

Figure 1 shows HRSEM micrographs of the prepared MWCNTs. It is possible to observe the perpendicular upward growth of carbon nanotubes attached to Vycor tube with lengths of several microns. The MWCNTs present diameters from 50 to 110 nm.

HRSEM micrography of Pt/MWCNTs shows the surface of the MWCNTs decorated with small particles of Pt (bright particles), which are uniformly distributed along the carbon nanotubes (Fig. 2a). The TEM image of the Pt/MWCNTs (Fig. 2b) shows Pt particles with a spherical shape and homogeneous distribution over the surface of the carbon nanotubes. Similar results were observed on different areas of the sample. The metallic particle size distribution was obtained by measuring a representative number of particles (∼100 nanoparticles) and the average particle size was 6.5 ± 1.5 nm. However, this size is

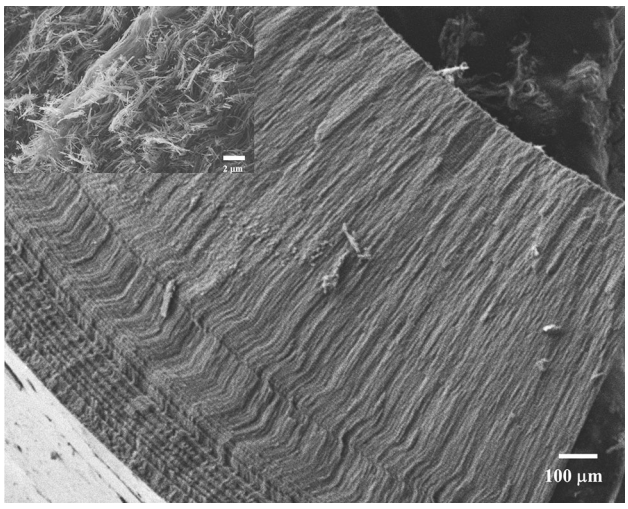

Fig. 1 HRSEM micrographs of MWCNTs prepared via chemical vapor deposition method; the *inset* plot shows the MWCNT at highest magnification

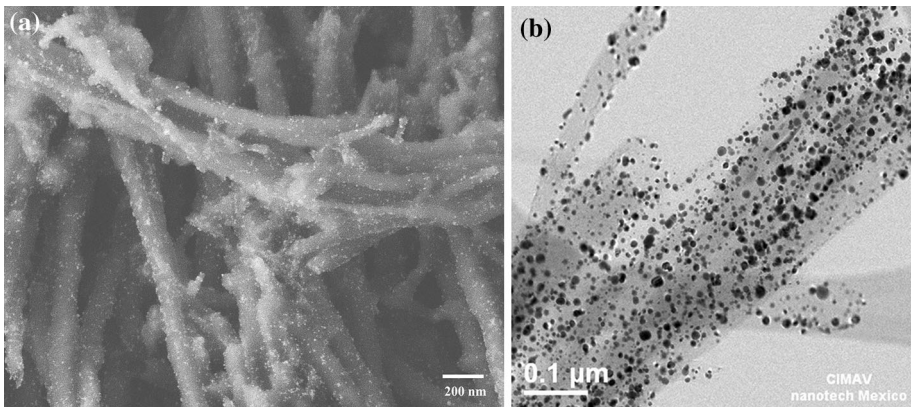

Fig. 2 Micrograph of platinum nanoparticles supported MWCNTs using **a** HRSEM at low voltage and **b** bright-field HRTEM

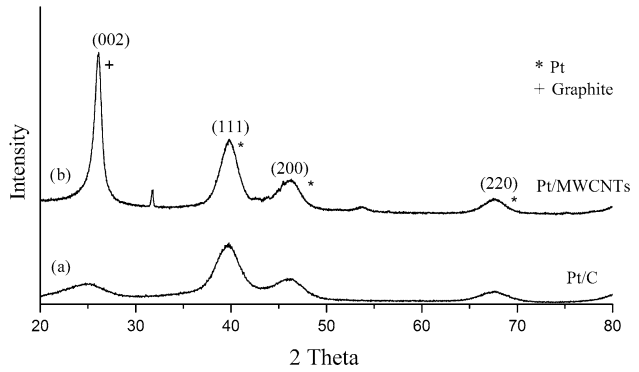

Fig. 3 X-ray diffraction patterns of: **a** Pt/C commercial and **b** Pt/MWCNTs prepared via colloidal synthesis. Miller index of each diffraction signal is denoted above each signal

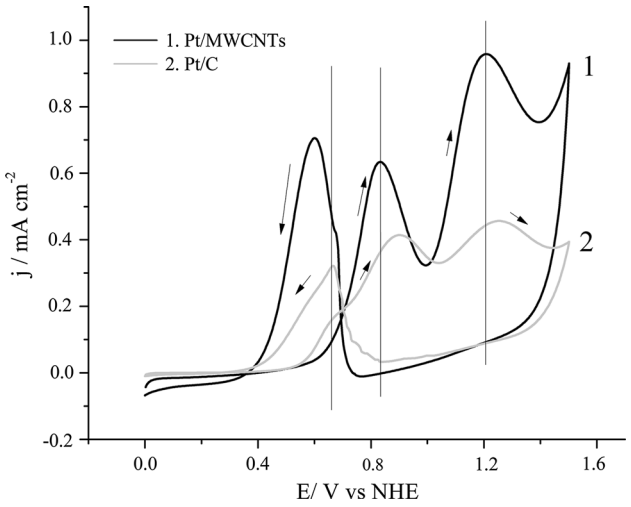

Fig. 4 Cyclic voltammograms on Pt/C and Pt/MWCNTs in 1.0 M CH_3CH_2OH + 0.5 M H_2SO_4 at a scan rate of 50 mV s^{-1}

greater than what has been reported as the ideal size of Pt catalysts for ethanol electro-oxidation [21]. EDS analyses of the MWCNTs showed a Pt content of 19.7 wt%, which concurs with the theoretical Pt loading (20 wt%).

Figure 3 illustrates the XRD patterns of the Pt/MWCNTs and Pt/C electrocatalysts. The diffraction peaks at $2\theta = 39.8$, 46.0, and 67.5 correspond to Pt (111), Pt (200), and Pt (220) of the Pt fcc phase (Card 4-0802) [22]. The corresponding peaks of the (002) and (004) planes of graphite 2H (Card 01-070-2057) appear at 26.2° and 53.9° 2θ. The reflection at 32° for the Pt/MWCNTs is attributed to residual sodium chloride [18]. The typical diffraction peaks which belong to FCC platinum can be clearly observed for both samples. The characteristic peaks of metallic Pt nanoparticles corresponding to the (111), (200), and (220) planes indicate that Pt has been reduced successfully.

3.2 Electrochemical measurements

Cyclic voltammograms for Pt/C and Pt/MWCNTs obtained in acid media and recorded at scan rate of 20 mV s^{-1} were reported in previous work [18]. The electrochemical active areas (EAA) were calculated from the peaks attributed to proton desorption from different Pt crystalline planes. EAA were 151 m^2 g^{-1} and 98 m^2 g^{-1} for Pt/MWCNTs and Pt/C, respectively. Cyclic voltammetry results indicate that both materials displayed the same electrochemical processes. However, higher current density was registered with the MWCNT-supported material.

Figure 4 presents the CV profiles recorded at a scan rate of 10 mV s^{-1} in 1.0 M ethanol +0.5 M H_2SO_4 solution and normalized with respect to the catalytic active area. In the scan towards positive potentials, two principal oxidation processes are observed. The first one corresponds to acetaldehyde formation, beginning at 0.38 V, with a maximum at 0.9 V for Pt/C [23]. The second one, associated with acetic acid formation, starts at 1 V with a maximum peak potential at 1.2 V. A shoulder is observed at 0.7 V, corresponding to the electrochemical activation of water. Finally, oxygen evolution occurs at 1.3 V. In the reverse scan, towards negative potentials, anodic currents are observed between 0.8 and 0.5 V. The slope change in

this process is characteristic of the oxidation of adsorbed organic species. Two oxidation processes are observed, at 0.66 V and at 0.58 V, which could be attributed to two different adsorbed species.

In the Pt/MWCNTs sample, a displacement to lower potentials is evident for peaks 1 and 2 compared with Pt/C. Furthermore, the highest current density for the ethanol oxidation reaction was observed with Pt/MWCNTs material. The first peak for synthesized material was 0.63 mA cm^{-2}, compared with 0.41 mA cm^{-2} for Pt/C. The same tendency was also observed for the other two peaks. A good electrocatalyst must fulfill at least two requirements: 1) high current density and 2) lower potentials for the corresponding electrochemical process. According to this, Pt/MWCNTs present higher ethanol electro-oxidation activity than Pt/C. In the scan towards negative potentials, the adsorbed species oxidation peak presents different behaviors. The main peak potential was observed at 0.60 V and a shoulder at 0.67 V, which could be explained by a different intermediate formation rate with the MWCNT-supported material. It is possible that a modification in the interaction between the active phase and support could change the mechanism of intermediate formation selectivity.

Figure 5 compares the single direct ethanol fuel cell performance using the synthesized Pt/MWCNTs and commercial Pt/C as anode electrocatalysts. In both cells, PtRu/C was used as the cathode electrocatalyst. The open-circuit potential for Pt/MWCNTs is 1.04 V, but there is a rapid initial drop in the cell voltage to 0.7 V, which is still higher than Pt/C (0.65 V). This cell voltage drop could be caused by the slow ethanol electro-oxidation reaction occurring at the Pt active sites. From the polarization and power curves, it is evident that the MWCNT-supported material offers a more effective catalytic behavior for the ethanol electro-oxidation reaction than Pt/C. A maximum power density of 3.14 mW cm^{-2} was observed with Pt/MWCNTs compared to 0.95 mW cm^{-2} for Pt/C.

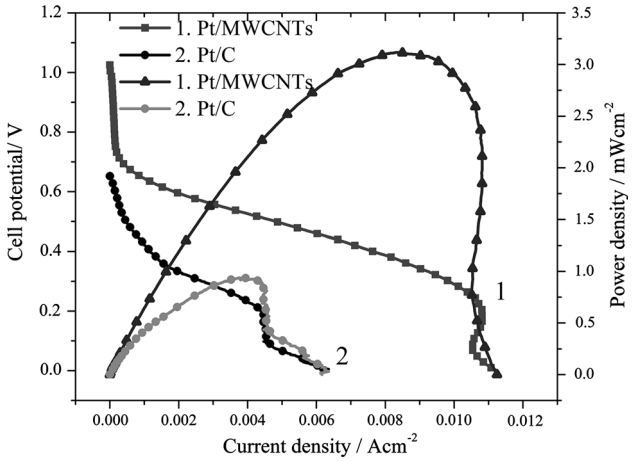

Fig. 5 Polarization curves for DEFC with anode (Pt/MWNTs or Pt/C) and cathode (PtRu/C) electrocatalyst loading of 1 mgPt cm^{-2}. Feed: anode, 1.0 M CH_3CH_2OH at 1.5 mL min^{-1}; cathode, air at 140 mL min^{-1}

4 Conclusions

Pt electrocatalyst supported on MWCNTs for DEFC applications was successfully prepared using the colloidal method. The colloidal dispersion was used to deposit Pt nanoparticles on the surface of the MWCNTs. Good Pt nanoparticle dispersion, desired composition, and excellent morphology were obtained. The particles on the MWCNTs had a size of around 6.5 ± 1.5 nm. X-ray diffraction showed diffraction peaks corresponding to graphite, and metallic Pt. Carbon nanotubes increased the activity of the Pt electrocatalyst and modified the selectivity of intermediate species, mainly favoring acetic acid production. The same was observed in the reverse scan oxidation peak, with changes to the two adsorbed intermediate species oxidation current intensities. Activity tests in a DEFC were consistent with CV analysis. Single fuel cell tests indicate that the MWCNT-supported Pt anode shows competitive performance in comparison with the conventional Pt/C-based electrode.

Acknowledgments The authors wish to thank Daniel Moreno for the electrochemical characterizations and acknowledge the financial support received from CONACYT-213373 and TNM under Grant No. 5201.14-P. The authors are also grateful for the support from the Laboratorio Nacional de Nanotecnología (CIMAV). B. Escobar wishes to thank the CONACYT-Cátedras program.

References

1. Oh Y, Kim S-K, Peck D-H, J-s Jang, Kim J, Jung D-H (2014) Improved performance using tungsten carbide/carbon nanofiber based anode catalysts for alkaline direct ethanol fuel cells. Int J Hydrog Energy 39:15907–15912. doi:10.1016/j.ijhydene.2014.02.010
2. Song SQ, Zhou WJ, Zhou ZH, Jiang LH, Sun GQ, Xin Q, Leontidis V, Kontou S, Tsiakaras P (2005) Direct ethanol PEM fuel cells: the case of platinum based anodes. Int J Hydrog Energy 30:995–1001. doi:10.1016/j.ijhydene.2004.11.006
3. Figueiredo MC, Sorsa O, Doan N, Pohjalainen E, Hildebrand H, Schmuki P, Wilson BP, Kallio T (2015) Direct alcohol fuel cells: increasing platinum performance by modification with sp-group metals. J Power Sources 275:341–350. doi:10.1016/j.jpowsour.2014.11.034
4. He Z, Chen J, Liu D, Zhou H, Kuang Y (2004) Electrodeposition of Pt–Ru nanoparticles on carbon nanotubes and their electrocatalytic properties for methanol electrooxidation. Diam Relat Mater 13:1764–1770. doi:10.1016/j.diamond.2004.03.004
5. Alzate V, Fatih K, Wang H (2011) Effect of operating parameters and anode diffusion layer on the direct ethanol fuel cell performance. J Power Sources 196:10625–10631. doi:10.1016/j.jpowsour.2011.08.080

6. Basri S, Kamarudin SK, Daud WRW, Yaakub Z (2010) Nanocatalyst for direct methanol fuel cell (DMFC). Int J Hydrog Energy 35:7957–7970. doi:10.1016/j.ijhydene.2010.05.111
7. Kamavaram V, Veedu V, Kannan AM (2009) Synthesis and characterization of platinum nanoparticles on in situ grown carbon nanotubes based carbon paper for proton exchange membrane fuel cell cathode. J Power Sources 188:51–56. doi:10.1016/j.jpowsour.2008.11.084
8. Tsai M-C, Yeh T-K, Tsai C-H (2011) Methanol oxidation efficiencies on carbon-nanotube-supported platinum and platinum–ruthenium nanoparticles prepared by pulsed electrodeposition. Int J Hydrog Energy 36:8261–8266. doi:10.1016/j.ijhydene.2011.03.107
9. Wang X, Li W, Chen Z, Waje M, Yan Y (2006) Durability investigation of carbon nanotube as catalyst support for proton exchange membrane fuel cell. J Power Sources 158:154–159. doi:10.1016/j.jpowsour.2005.09.039
10. Li W, Wang X, Chen Z, Waje M, Yan Y (2005) Carbon nanotube film by filtration as cathode catalyst support for proton-exchange membrane fuel cell. Langmuir 21:9386–9389. doi:10.1021/la051124y
11. Yang G-W, Gao G-Y, Zhao G-Y, Li H-L (2007) Effective adhesion of Pt nanoparticles on thiolated multi-walled carbon nanotubes and their use for fabricating electrocatalysts. Carbon 45(15):3036–3041. doi:10.1016/j.carbon.2007.06.021
12. Liu Z-L, Huang R, Deng Y-J, Chen D-H, Huang L, Cai Y-R, Wang Q, Chen S-P, Sun S-G (2013) Catalyst of Pt nanoparticles loaded on multi-walled carbon nanotubes with high activity prepared by electrodeposition without supporting electrolyte. Electrochim Acta 112:919–926. doi:10.1016/j.electacta.2013.05.139
13. Jiang Z, Z-j Jiang, Meng Y (2011) High catalytic performance of Pt nanoparticles on plasma treated carbon nanotubes for electrooxidation of ethanol in a basic solution. Appl Surf Sci 257:2923–2928. doi:10.1016/j.apsusc.2010.10.091
14. Cai J, Huang Y, Huang B, Zheng S, Guo Y (2014) Enhanced activity of Pt nanoparticle catalysts supported on manganese oxide-carbon nanotubes for ethanol oxidation. Int J Hydrog Energy 39:798–807. doi:10.1016/j.ijhydene.2013.10.108
15. Rodriguez JR, Félix RM, Reynoso EA, Gochi-Ponce Y, Gómez YV, Moyado SF, Alonso-Núñez G (2014) Synthesis of Pt and Pt-Fe nanoparticles supported on MWCNTs used as electrocatalysts in the methanol oxidation reaction. J Energy Chem 23:483–490. doi:10.1016/S2095-4956(14)60175-3
16. Guinel MJF, Brodusch N, Verde-GÓMez Y, Escobar-Morales B, Gauvin R (2013) Multi-walled carbon nanotubes decorated by platinum catalyst nanoparticles—examination and microanalysis using scanning and transmission electron microscopies. J Microsc 252:49–57. doi:10.1111/jmi.12067
17. Escobar Morales B, Gamboa SA, Pal U, Guardián R, Acosta D, Magaña C, Mathew X (2010) Synthesis and characterization of colloidal platinum nanoparticles for electrochemical applications. Int J Hydrog Energy 35:4215–4221. doi:10.1016/j.ijhydene.2010.01.040
18. Escobar B, Barbosa R, Miki Yoshida M, Verde Gomez Y (2013) Carbon nanotubes as support of well dispersed platinum nanoparticles via colloidal synthesis. J Power Sources 243:88–94. doi:10.1016/j.jpowsour.2013.05.123
19. Camara GA, Iwasita T (2005) Parallel pathways of ethanol oxidation: the effect of ethanol concentration. J Electroanal Chem 578:315–321. doi:10.1016/j.jelechem.2005.01.013
20. Zhao H, Li L, Yang J, Zhang Y (2008) Nanostructured polypyrrole/carbon composite as Pt catalyst support for fuel cell applications. J Power Sources 184:375–380. doi:10.1016/j.jpowsour.2008.03.024
21. Sun C-L, Tang J-S, Brazeau N, Wu J-J, Ntais S, Yin C-W, Chou H-L, Baranova EA (2015) Particle size effects of sulfonated graphene supported Pt nanoparticles on ethanol electrooxidation. Electrochim Acta 162:282–289. doi:10.1016/j.electacta.2014.12.099
22. Weijiang Zhou ZZ, Song Shuqin, Li Wenzhen, Gongquan Sun PT, Xin Qin (2003) Pt based anode catalysts for direct ethanol fuel cells. Appl Catal B 46:273–285
23. Lamy C, Belgsir EM, Léger JM (2001) Electrocatalytic oxidation of aliphatic alcohols: application to the direct alcohol fuel cell (DAFC). J Appl Electrochem 31:799–809. doi:10.1023/a:1017587310150